# Observation of field-induced charge carriers in high-mobility organic transistors of a thienothiophene-based small molecule: Electron spin resonance measurements

Hisaaki Tanaka,[1] Masato Kozuka,[1] Shun-ichiro Watanabe,[1] Hiroshi Ito,[1] Yukihiro Shimoi,[2]
Kazuo Takimiya,[3] and Shin-ichi Kuroda[1]

[1]*Department of Applied Physics, Nagoya University, Chikusa-ku, Nagoya 464-8603, Japan*
[2]*Nanosystem Research Institute (NRI), National Institute of Advanced Industrial Science and Technology (AIST), 1-1-1 Umezono, Tsukuba, Ibaraki 305-8568, Japan*
[3]*Institute for Advanced Materials Research, Hiroshima University, Higashi-Hiroshima 739-8530, Japan*

Electron spin resonance (ESR) measurements are performed on field-induced charge carriers in high-mobility organic transistors of polycrystalline dioctylbenzothieno[2,3-b]benzothiophene ($C_8$-BTBT) films. The angular dependences of the ESR spectra are well fitted by orthorhombic $g$ values with the largest component of $g_Y = 2.0110$ nearly parallel to the normal direction of the substrate but tilted by $5°$. The results indicate a highly organized end-on alignment of $C_8$-BTBT molecules at the device interface. The ESR linewidth exhibits motional narrowing down to 4 K, providing microscopic evidence for high carrier mobilities within the crystalline domains of $C_8$-BTBT.

Organic field-effect transistors (OFETs) using $\pi$-conjugated molecules are attracting much attention due to their potential applications for low-cost, flexible, and large-area electronic circuits.[1,2] It is widely accepted that the degree of molecular ordering greatly affects the efficiency of charge transport in these devices. In the case of polythiophene-based polymer transistors, for example, it has been reported that the incorporation of a fused thiophene ring, thieno[3,2-b] thiophene, into the backbone drastically improves the carrier mobility ($\mu$) to as high as 1 cm$^2$/Vs due to the formation of highly ordered, large crystalline domains.[3] The air stability of the device characteristics has been improved as well due to the larger ionization potential realized by the incorporated fused units. Recently, a series of small molecules 2,7-dialkyl[1]benzothieno[3,2-b][1]-benzothiophene [$C_n$-BTBT; shown in Fig. 1(a)], have been synthesized, which exhibit high mobility.[4,5] In this system, relatively short sulfur-sulfur contacts between the herringbone-packed molecules, shown in Fig. 1(b), promote the delocalization of carriers. As a result, mobility as high as 5 cm$^2$/Vs has been reported for solution-processed thin films of $C_8$-BTBT ($n = 8$).[6] Furthermore, a bandlike transport mechanism is suggested from the temperature dependence of mobility in FETs using $C_8$-BTBT single crystals.[7] The bandlike nature of the charge transport has also been observed in polycrystalline thin films of another thienothiophene-based small molecule, dinaptho[2,3-b:2′3′-f]thieno[3,2-b]thiophene (DNTT),[8] from Hall effect measurements.[9] In general, however, carrier trapping due to grain boundaries in thin films masks the intrinsically high carrier mobility inside the ordered domain, especially at low temperatures.[9,10] Thus, it is indispensable to observe charge carriers directly by using microscopic methods in order to clarify their low-temperature behaviors.

Field-induced electron spin resonance (FI-ESR) spectroscopy, developed by our group, is a particularly suitable method for this purpose owing to its high sensitivity for detection of the spin of accumulated carriers at the insulator interface.[11] So far, FI-ESR measurements have been reported in thin-film transistors of regioregular poly(3-alkylthiophene)

(Refs. 11–14) and pentacene,[15–17] giving microscopic information such as the spin-charge relation, the wave function of the charge carriers, and the local molecular orientation at the device interface. Another important feature that can be clarified by this method is the motion of the accumulated carriers obtained from the motional narrowing of the ESR linewidth.[11,16,17] A close correspondence between the motionally narrowed ESR linewidth and the macroscopic FET mobility has been demonstrated by a recent FI-ESR study of rubrene single-crystal transistors[18] based on the multiple trap and release model.[2,10] On the other hand, single-crystal samples often crack on cooling due to the mismatch of thermal expansion between the samples and substrates, preventing low-temperature measurements, whereas in the case of polycrystalline thin films, carriers tend to be deeply trapped at low temperatures, as is the case in pentacene FETs.[16,17] Direct observation of mobile charge carriers in OFETs at low temperatures has not been reported yet.

In this Rapid Communication, we report on FI-ESR measurements in polycrystalline OFETs of a thienothiophene-based small molecule $C_8$-BTBT exhibiting $\mu$ greater than 1 cm$^2$/Vs. ESR spectra, observed down to 4 K, show clear angular dependences with resolved peaks as the external field is rotated from the normal direction of the substrate. They are fitted well by orthorhombic $g$ values with the largest component of $g_Y = 2.0110$ nearly parallel to the normal direction but tilted by $5°$, providing evidence for a highly organized end-on orientation of $C_8$-BTBT molecules at the device interface. Furthermore, the ESR linewidth shows a temperature-dependent motional narrowing due to thermal motion of carriers. These results demonstrate the high carrier mobility inside crystalline domains even at 4 K in such polycrystalline OFETs of a thionothiophene-based molecule.

The FET devices were fabricated on $n^+$-Si substrates with SiO$_2$ gate insulators.[12,13] $C_8$-BTBT thin films with typical thickness of 80 nm were vapor deposited on an $n^+$-Si wafer (10–20 Ωcm, ⟨100⟩ axis) with 300-nm-thick thermally grown SiO$_2$ treated with hexamethyldisilazane. Au electrodes were vapor deposited on the film to form the top-contact FET
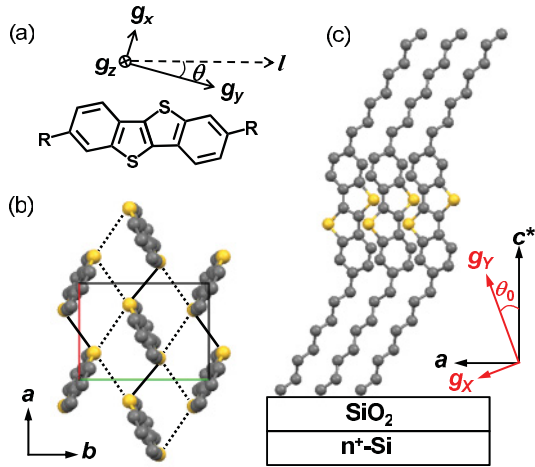
FIG. 1. (Color online) (a) Chemical structure of $C_n$-BTBT with the principal axes of the $g$ tensor. $\theta$ denotes the angle between the $g_y$ axis and the molecular long axis ($l$) connecting 2,7 carbon atoms. (b) Crystal structure of $C_8$-BTBT viewed along the $c$ axis (Ref. 5). The octyl group and hydrogen atoms are omitted. Solid and dashed lines represent the intermolecular sulfur-sulfur contacts within the *ab* plane. (c) Schematic illustration of molecular ordering on the $SiO_2$ substrate viewed along the $b$ axis. $\theta_0$ denotes the angle between the $g_Y$ axis and the $c^*$ axis of the crystallite.

geometry. Typical dimensions of the devices were channel lengths $L$ of 0.3 or 1.0 mm and channel widths $W$ of $\sim$20 mm. FET characteristics were measured by using a Keithley 2612 source measure unit. We obtained the typical FET characteristics as reported for $C_n$-BTBT FETs;[5] the average mobility in the saturation regime was $\mu = 1.1$ cm$^2$/Vs with the maximum value of 4.3 cm$^2$/Vs at room temperature, and the threshold voltage was $-30 \pm 10$ V. The mobility was obtained without correcting for the effect of contact resistance. ESR measurements were performed by using a Bruker E-500 spectrometer equipped with an Oxford ESR 900 gas-flow-type cryostat. The source and drain electrodes were short-circuited in the FI-ESR measurements to form a metal-insulator-semiconductor (MIS) capacitor structure. The magnetic field was determined with the accuracy of $\pm$0.01 G by using a nuclear magnetic resonance teslameter.

Figure 2(a) shows the temperature dependence of the first-derivative FI-ESR signal of the $C_8$-BTBT FET having room-temperature mobility of 1.9 cm$^2$/Vs. The applied gate bias is $V_g = -80$ V and the external magnetic field ($H$) is perpendicular to the substrate. The gate bias was applied at room temperature prior to the cooling. A single intense signal is observed around $g = 2.0109$ at 4 K, which is ascribed to the $\pi$ electrons of $C_8$-BTBT. The spin concentration was estimated to be $1.3 \times 10^{12}$ spins/cm$^2$. The observed $g$ value exhibits a relatively large shift from the free-electron value of $g_e = 2.0023$, compared with rubrene or pentacene devices, which have the maximum $g$ value of $\sim$2.003 along the molecular long axis.[15,16,18] The large $g$ shift may be reasonably ascribed to the large spin-orbit coupling of the sulfur atoms incorporated in the BTBT molecule. This fact has also been confirmed by a density functional theory (DFT) calculation of the $g$ value for the BTBT molecule.[19] Furthermore, the large spin-orbit coupling of sulfur atoms tends to cause a prominent broadening
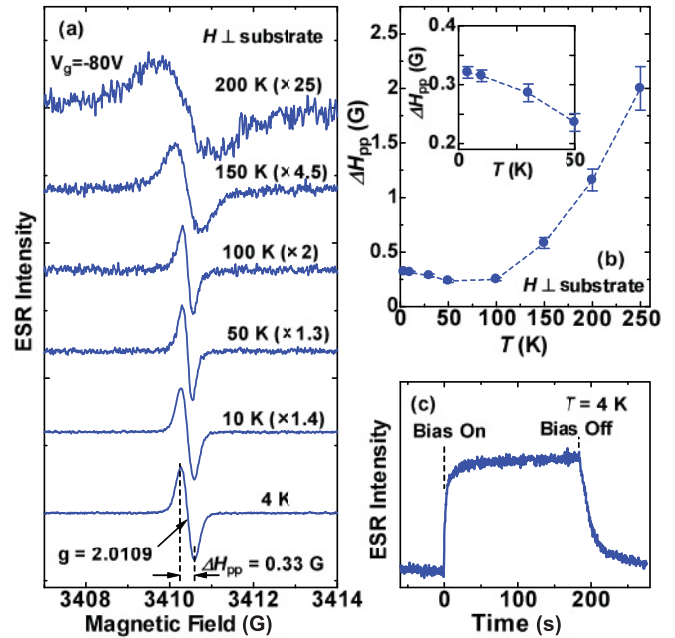


FIG. 2. (Color online) Temperature dependence of (a) first-derivative FI-ESR spectra and (b) peak-to-peak linewidth obtained for a $C_8$-BTBT FET. The applied gate voltage is $-80$ V and the external field is perpendicular to the substrate. The inset shows the magnified plot of the linewidth below 50 K. (c) Transient response of FI-ESR intensity upon applying gate bias of $-80$ V at 4 K.

of the ESR linewidth above 100 K as shown in Figs. 2(a) and 2(b) through the shortening of the spin-lattice relaxation time. As a result, the FI-ESR signal could not be observed at room temperature in the $C_8$-BTBT FETs, in sharp contrast to rubrene or pentacene devices.[15–18]

Below 100 K, on the other hand, the ESR linewidth shows gradual narrowing as the temperature is raised, as shown specifically in the inset of Fig. 2(b) below 50 K. This behavior can be reasonably ascribed to the motional narrowing of the hyperfine-originated ESR linewidth due to the thermal motion of charge carriers. Such temperature-dependent narrowing has also been reported in FI-ESR studies of pentacene FETs having mobility of 0.6 cm$^2$/Vs.[16,17] A marked difference in the present case, however, is that the narrowing effect was observed down to 4 K. In the pentacene case, the linewidth was found to be temperature independent below 50 K due to carrier trapping. To confirm the motional narrowing effect in the present device, we performed a microwave power saturation experiment at 4 K. The ESR linewidth indeed becomes broader for larger microwave power due to power saturation, which is a typical behavior of a motionally narrowed spectrum.[17,20] The presence of mobile carriers enables carrier injection at low temperatures, as directly evidenced by the transient response of the FI-ESR signal at 4 K [Fig. 2(c)]. The relatively slow response time in the figure may be due to the presence of trap sites in the carrier path of the MIS structure. It should also be pointed out that the output currents of the present FETs were observed only above 60 K due to the trapping at grain boundaries in the FET channel, as in the FETs of polycrystalline DNTT.[9]

The observed narrowed linewdth of $\Delta H_{1/2} \sim 0.39$ G ($\sim$0.45 G when averaged with respect to the anisotropy) at

4 K provides the basis for discussing carrier dynamics; $\Delta H_{1/2}$ denotes the full width at half maximum. For this purpose, we first examine the static linewidth $\Delta H_d$. The static linewidth, dominated by the proton hyperfine interaction, depends on the number of interacting protons ($n$) as $\Delta H_d \propto n^{-1/2}$.[15] When a carrier is confined in one BTBT molecule, the static width is expected to be about 5 G based on the DFT calculation. On the other hand, the carrier wave function is supposed to extend over several molecules in the ordered domain as suggested by the bandlike nature of charge transport[9,15] in the single-crystal device.[7] If we assume the extension of the wave function to be about ten molecules as in the pentacene FET, the static linewidth becomes ~1.6 G. Note that this value is clearly larger than the observed $\Delta H_{1/2}$. According to the conventional motional narrowing theory, by using $\Delta H_{1/2}$ and $\Delta H_d$, we can estimate the carrier trapping time ($\tau_{\mathrm{tr}}$) *within* a crystalline domain, or the time that a carrier spends within a trap site in other words, by the relation[18,21] $\Delta H_{1/2} \cong \gamma(\Delta H_d)^2 \tau_{\mathrm{tr}}$, where $\gamma$ denotes the gyromagnetic ratio of $\pi$ electrons. $\Delta H_{1/2} = 0.45$ G and $\Delta H_d \sim 1.6$ G results in $\tau_{\mathrm{tr}} \sim 60$ ns at 4 K. For higher temperatures, the narrower linewidth shown in the inset of Fig. 2(b) indicates the lower value of $\tau_{\mathrm{tr}}$, presumably reflecting higher mobility. Although the temperature dependence of $\tau_{\mathrm{tr}}$ is an interesting subject for clarification of the microscopic carrier mobility, more detailed analyses employing various theoretical models are left open for further studies.

These results indicate the presence of crystalline domains having high carrier mobilities that should be associated with a high degree of molecular order at the device interface. ESR spectroscopy can provide direct information about molecular orientation at the interface through the anisotropic $g$ values of the $\pi$ electrons. Dashed lines in Fig. 3(a) show the angular
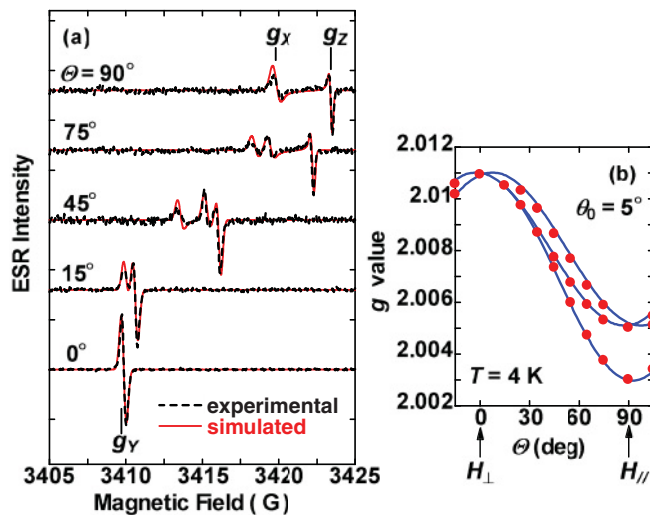


FIG. 3. (Color online) (a) Angular dependence of first-derivative FI-ESR spectra at 4 K with the gate bias of $-80$ V. The dashed and solid curves represent the experimental and simulated spectra, respectively. The inclination angle of the $g_Y$ component from the $c^*$ axis is $\theta_0 = 5°$. The magnetic fields corresponding to $g_X$, $g_Y$, and $g_Z$ are shown. See text for other details of the simulation. (b) Angular dependence of $g$ values of the split lines. Solid curves represent the calculated curves for $\theta_0 = 5°$.

dependence of the FI-ESR signal of the $C_8$-BTBT FET at 4 K. $\Theta$ denotes the angle between the external magnetic field and the substrate normal. The FI-ESR spectra taken parallel and perpendicular to the substrate are typical for a system having orthorhombic $g$ values with a nearly uniaxial molecular orientation along the substrate normal, giving a single sharp spectrum at $\Theta = 0°$ from one $g$ component, whereas two peaks at $\Theta = 90°$ correspond to the other two components. The splitting at $\Theta = 90°$ indicates that the in-plane orientation is random, which is to be expected for vacuum-deposited thin films. A striking feature, on the other hand, is the appearance of triply split structures at intermediate angles. This provides direct evidence for a small but finite tilt of the principal $g$ axis from the normal direction of the substrate, because in such a case the maximum $g$ value component should appear at an intermediate angle, resulting in the splitting of lines. Then the analysis of the observed spectra using an ESR spectrum simulation determines the detailed molecular orientation as discussed below.

We set the principal axes ($x,y,z$) of the $g$ tensor for each molecule as shown in Fig. 1(a), where the $z$ direction is parallel to the $p\pi$ orbital axis. $\theta$ denotes the angle between the $y$ axis and the molecular long axis ($l$) connecting the 2,7 carbon atoms. According to the DFT calculations, the largest $g$ shift appears in the $y$ direction, dominating the ESR spectrum at $\Theta = 0$ with the largest $g$ value. Thus, the $l$ vector is nearly parallel to the substrate normal when $\theta$ is small. This result allows us to adopt the herringbone-packed molecular ordering in Fig. 1(b) at the interface in the first approximation, as in the case of a bulk thin film. In this case, the crystallographic $ab$ plane lies on the substrate plane,[5] with the result that the $c^*$ axis is parallel to the substrate normal. As shown in Fig. 1(b), a unit cell of $C_8$-BTBT contains two equivalent molecules with different molecular orientations. A spin extending over both molecules provides a single $g$ tensor in a crystallite which reflects the crystal symmetry. We set its principal axes ($X,Y,Z$) as schematically shown in Fig. 1(c). Because of the $C_2$ screw axis along the $b$ axis, the $Z$ axis should be parallel to the $b$ axis. The $X$ and $Y$ axes lie in the $ac^*$ plane with an inclination angle $\theta_0$ between the $c^*$ and $Y$ axes. We stress that $\theta_0$ remains finite in the crystallite since the tilting of the $y$ axis (and $x$ axis) of the herringbone pair is *common* in this plane. Meanwhile, the tilting is canceled out in the $bc^*$ plane.

When an external magnetic field is applied to the system with the direction cosines of ($L,M,N$) to the crystallite $g$ axes ($X,Y,Z$), the $g$ value is given by $g^2 = g_X^2 L^2 + g_Y^2 M^2 + g_Z^2 N^2$. The corresponding resonance field is given by $H_{\mathrm{res}} = h\nu/g\mu_B$, where $h\nu$ shows the energy of the microwave photon quanta and $\mu_B$ denotes the Bohr magneton. We use a Gaussian derivative[22] for each $H_{\mathrm{res}}$ with the peak-to-peak linewidth of $\Delta H_{\mathrm{pp}}^2 = \Delta H_X^2 L^2 + \Delta H_Y^2 M^2 + \Delta H_Z^2 N^2$.[15] Since the in-plane orientation of the grain is random, these spectra are summed over all in-plane orientations at each angle $\Theta$. We use $g_i$, $\Delta H_i$ ($i = X,Y,Z$), and $\theta_0$ as fitting parameters and their fitted values are $g_X = 2.0050$, $g_Y = 2.0110$, $g_Z = 2.0030$, $\Delta H_X = 0.35$ G, $\Delta H_Y = 0.25$ G, $\Delta H_Z = 0.15$ G, and $\theta_0 = 5° \pm 1°$. The calculated spectra are shown in Fig. 3(a) (solid curves). Figure 3(b) shows the angular dependence of $g$ values for all the split lines together with the simulated results using

the above parameter values. The important fact is that the finite value of $\theta_0$ excellently reproduces the triply split lines at the intermediate angles as shown in Fig. 3(a), whereas if we set $\theta_0 = 0$, only two peaks appear, as expected for the typical uniaxial orientation. The accuracy of $\theta_0$ is as high as $1°$ because the positions of the split lines are sensitive to $\theta_0$ due to the large $g$ shift of the $Y$ component.

Finally, we discuss the origin of the finite $\theta_0$ value. According to x-ray structure analyses,[5] the thienothiophene planes tilt by about $1.6°$ from the $c^*$ axis in an alternating manner with its herringbone-packed counterpair, as shown in Fig. 1(b). There is also a small tilt of the vector $l$ of less than $1°$ within the molecular plane with respect to the $c^*$ axis. However, these structural tilts are too small to explain the $\theta_0$ determined above. According to the DFT calculations on an isolated BTBT molecule, the $g_y$ axis inclines from the molecular long axis as shown in Fig. 1(a). Although the absolute magnitude of $\theta$ ($\sim 30°$) is larger than the obtained value of $\theta_0$, this effect explains the origin of the triply split signal. The discrepancy in the inclination angle may be improved if we consider the spatial extension of the wave functions over molecules in the calculation. Therefore, the present results unambiguously indicate that the molecular long axis stands on the substrate plane at the insulator interface to form the two-dimensional network of the $\pi$ stacking, resulting in high charge carrier mobility within the crystalline domains.

In summary, we clearly observed the motion of field-induced charge carriers at 4 K in polycrystalline thin films of $C_8$-BTBT through the motional narrowing of the FI-ESR spectra. The mobile carriers arise from highly ordered crystalline domains at the insulator interface, as directly demonstrated from the angular dependence of the FI-ESR signal. These results indicate that high-mobility carriers exist at low temperatures in the crystalline domains in thin-film FETs of a thienothiophene-based molecule.

[1] H. Sirringhaus, Adv. Mater. **17**, 2411 (2005).

[2] M. E. Gershenson, V. Podzorov, and A. F. Morpurgo, Rev. Mod. Phys. **78**, 973 (2006).

[3] I. McCulloch, M. Heeney, C. Bailey, K. Genevicius, I. MacDonald, M. Shkunov, D. Sparrowe, S. Tierney, R. Wagner, W. Zhang, M. L. Chabinye, R. J. Kline, M. D. McGehee, and M. F. Toney, Nature Mater. **5**, 328 (2006).

[4] H. Ebata, T. Izawa, E. Miyazaki, K. Takimiya, M. Ikeda, H. Kuwabara, and T. Yui, J. Am. Chem. Soc. **129**, 15732 (2007).

[5] T. Izawa, E. Miyazaki, and K. Takimiya Adv. Mater. **20**, 3388 (2008).

[6] T. Uemura, Y. Hirose, M. Uno, K. Takimiya, and J. Takeya, Appl. Phys. Express **2**, 111501 (2009).

[7] C. Liu, T. Minari, X. Lu, A. Kumatani, K. Takimiya, K. Tsukagoshi, Adv. Mater. **23**, 523 (2011).

[8] T. Yamamoto and K. Takimiya, J. Am. Chem. Soc. **129**, 2224 (2007).

[9] M. Yamagishi, J. Soeda, T. Uemura, Y. Okada, Y. Takatsuki, T. Nishikawa, Y. Nakazawa, I. Doi, K. Takimiya, and J. Takeya, Phys. Rev. B **81**, 161306(R) (2010).

[10] V. Podzorov, E. Menard, A. Borissov, V. Kiryukhin, J. A. Rogers, and M. E. Gershenson, Phys. Rev. Lett. **93**, 086602 (2004).

[11] K. Marumoto, Y. Muramatsu, Y. Nagano, T. Iwata, S. Ukai, H. Ito, S. Kuroda, Y. Shimoi, and S. Abe, J. Phys. Soc. Jpn. **74**, 3066 (2005).

[12] S. Watanabe, K. Ito, H. Tanaka, H. Ito, K. Marumoto, and S. Kuroda, Jpn. J. Appl. Phys. **46**, L792 (2007).

[13] H. Tanaka, S. Watanabe, H. Ito, K. Marumoto, and S. Kuroda, Appl. Phys. Lett. **94**, 103308 (2009).

[14] S. Watanabe, H. Tanaka, S. Kuroda, A. Toda, S. Nagano, T. Seki, A. Kimoto, and J. Abe, Appl. Phys. Lett. **96**, 173302 (2010).

[15] K. Marumoto, S. Kuroda, T. Takenobu, and Y. Iwasa, Phys. Rev. Lett. **97**, 256603 (2006).

[16] H. Matsui, T. Hasegawa, Y. Tokura, M. Hiraoka, and T. Yamada, Phys. Rev. Lett. **100**, 126601 (2008).

[17] H. Matsui, A. S. Mishchenko, and T. Hasegawa, Phys. Rev. Lett. **104**, 056602 (2010).

[18] K. Marumoto, N. Arai, H. Goto, M. Kijima, K. Murakami, Y. Tominari, J. Takeya, Y. Shimoi, H. Tanaka, S. Kuroda, T. Kaji, T. Nishikawa, T. Takenobu, and Y. Iwasa, Phys. Rev. B **83**, 075302 (2011).

[19] DFT calculations of the $g$ tensor for an isolated BTBT molecule were performed with the B3LYP functional and 6-31G(d) basis set. The alkyl chains are substituted with hydrogen atoms for simplicity. The calculations were carried out using the GAUSSIAN 09 software package [M. J. Frisch *et al.*, GAUSSIAN 09, rev. A. 02 (Gaussian, Inc., Wallingford, CT, 2009).

[20] A. Abragam, *The Principles of Nuclear Magnetism* (Clarendon Press, Oxford, 1961), Chap. 3.

[21] R. Kubo and K. Tomita, J. Phys. Soc. Jpn. **9**, 888 (1954).

[22] The line shape at 4 K, shown in Fig. 2(a), is not the pure Lorentzian of the completely homogeneous case but is more Gaussian-like except for the wing portion of the spectrum. A possible origin of this deviation may be the inhomogeneity caused by, for example, the small $g$ value distribution associated with misorientation of the molecular axis due to the roughness of the substrate surface, often observed in thin-film devices. Thus we use a Gaussian as the approximate line-shape function to take into account this effect.